Aerosol Optical Properties and Radiative Forcing of Extreme Wildfires with GCOM-C/SGLI

○Kazuhisa Tanada[1], Hiroshi Murakami[1], Tadahiro Hayasaka[1,2], Mayumi Yoshida[3]
1: Earth Observation Research Center (EORC), Japan Aerospace Exploration Agency (JAXA)
2: Center for Atmospheric and Oceanic Studies, Tohoku University
3: Remote Sensing Technology Center of Japan (RESTEC)

Introduction

It is known that wildfires not only damage land ecosystems, but also have a great impact on the atmospheric environment due to the release of large amounts of CO_2, aerosols and so on. Greenhouse gases such as CO_2 are well known to have positive radiative forcing, however, aerosols from biomass burning have both positive and negative radiative forcing potentials, which can perturb the global radiation balance. Therefore, it is important to investigate the aerosol optical properties of extreme wildfire events and estimate their radiative forcing in order to predict the future climatic impacts by biomass burning.

In this work, we analyze the world's wildfires in Amazon, Angola, Australia, California, Siberia, and Southeast Asia that occurred after 2018 with the GCOM-C satellite.

Data and Methods

①GCOM-C Satellite Data

・Ver.2 ARNP product (1 km resolution):
AOT (Aerosol Optical Thickness; 500 nm),
AE (Ångström exponent; 380-500 nm),
SSA (Single Scattering Albedo; 380 nm)

・Ver.1 WFRP product (250 m resolution)
WildFire Radiation Power, which is used to detect the hotspot locatoions.

②Copernicus Global Land Service: CGLS-LC100

・An annual dynamic global Land Cover product at 100 m spatial resolution.

③Japan Meteorological Agency / Global objective analysis data

・1 degree mesh GANAL data of relative humidity.

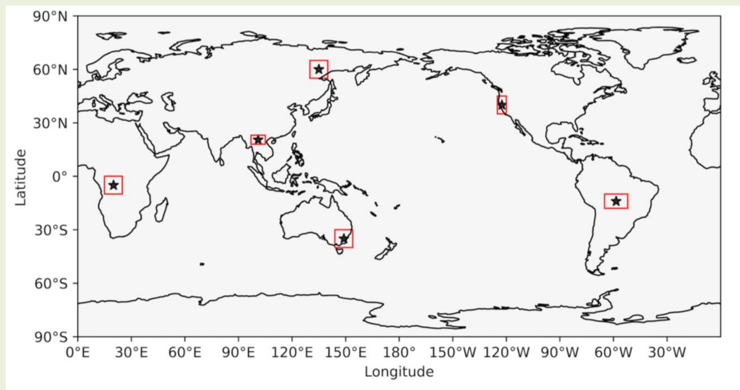

Fig. 1 The location of the wildfires

Table 1 The location and periods of the wildfires

Country / State	Longitude [°]	Latitude [°]	Month and Year
Amazon	52°W-65°W	10°S-18°S	Sep. 2020
Angola	15°E-25°E	0°S-10°S	Aug. 2020
Australia	144°E-154°E	30°S-40°S	Dec. 2019 - Jan. 2020
California	120°W-125°W	35°N-45°N	August 2018
			Jul. 2021
			Aug. 2020 - Sep. 2020
Southeast Asia	97°E-105°E	18°N-23°N	Mar. 2020 - Apr. 2020
Siberia	130°E-140°E	55°N-65°N	Aug. 2020
			Jul. 2021

Relative Humidity and Vegetation Type Dependences of Aerosol Optical Properties

First, we investigate the relationship between the aerosol optical properties and the local characteristics such as relative humidity and vegetation type. We found that there is a negative correlation between AE and relative humidity ($R2 = 0.42$, obtained by linear fitting). It means that the larger particle diameters are observed in regions with the higher relative humidity, which result suggests that the aerosols from biomass burning take up water and grow.

Next, we classified the fire events into two groups by their the most dominant vegetation types: needle-leaf forests in California and Siberia, and broadleaf forests in Amazon, Angola, Australia, and Southeast Asia. Along with this grouping, the linear fitting with the relationship between SSA and relative humidity for each group independently shows the decision coefficient of 0.98 (needle-leaf forest) and 0.23 (broadleaf forest), respectively. Therefore, we can assume that there is a positive correlation between SSA and relative humidity considering the vegetation difference.

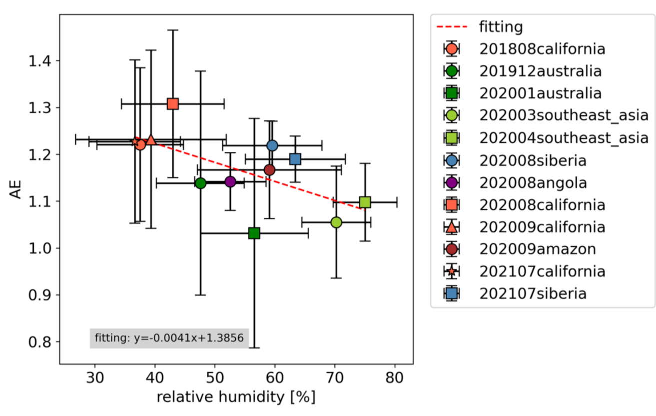

Fig. 2 AE vs. relative humidity for each fire event

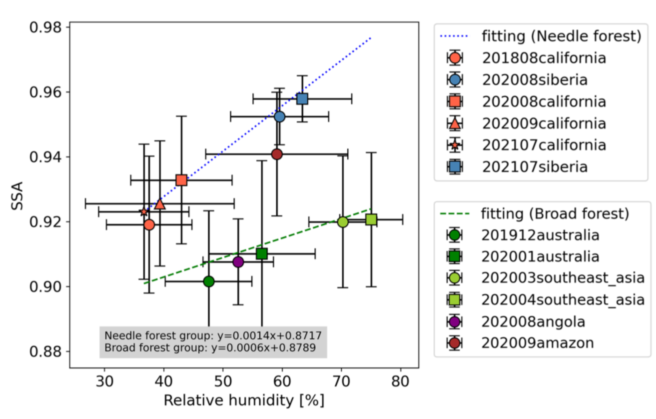

Fig. 3 SSA vs. relative humidity for each fire event

Aging Effect of Aerosols

We investigate the temporal variation of particle size for each fire event. The AE and SSA averages within each rectangle are plotted against the distance from the center coordinate of the first rectangle in the three right panels of Fig. 4. Because the distance from the hotspots is roughly proportional to the time elapsed since the smoke was generated, we can discuss the temporal changes in the properties of smoke particles in this analysis.

According to the results, we can see that the smoke particle size clearly increases (i.e. decrease in AE) with time in almost all locations, which indicates that the process of hygroscopic growth was observed. It is suggested that local differences in the characteristics of aerosols generated by wildfires are highly dependent on the relative humidity in each region and reflect the behavior of time-series changes in particle size.

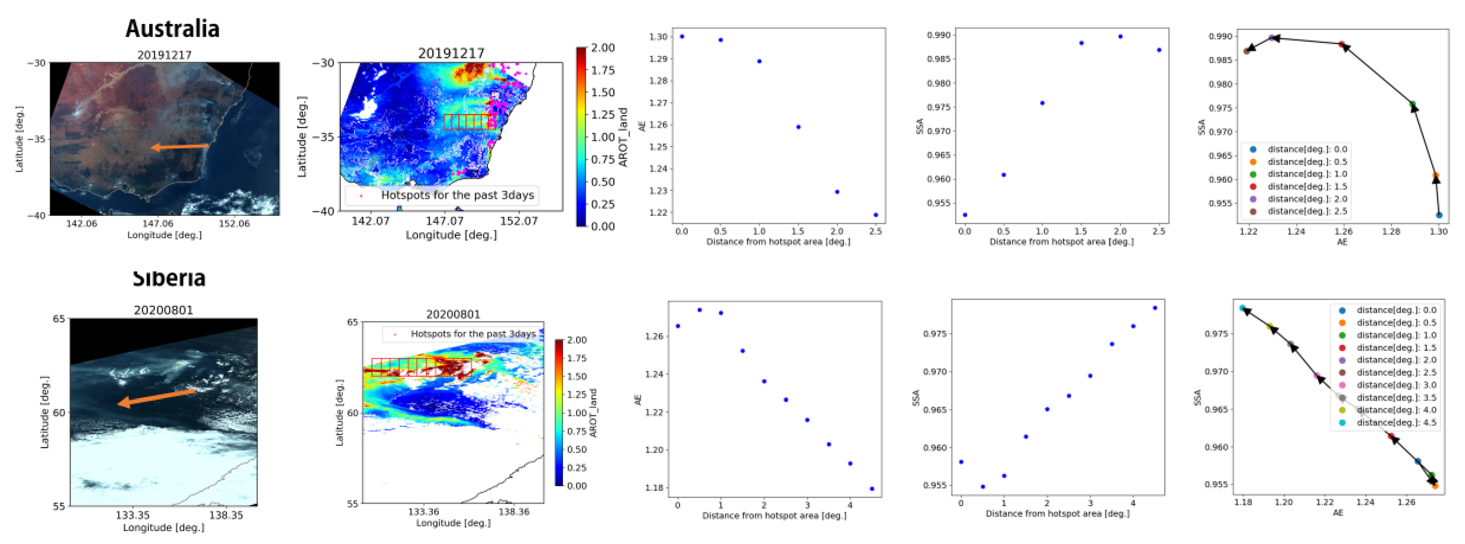

Fig. 4 RGB true, AOT, AE vs distance, SSA vs. distance, SSA vs. AE

Estimation of Aerosol Direct Radiative Forcing

In order to investigate the climate impacts for the different locations of wildfires, we estimated the shortwave radiative forcing as:

$$RF_{SW} = \pi[\int L_{TOA}^{\mathrm{base}}(\lambda)\, d\lambda - \int L_{TOA}^{\mathrm{fire}}(\lambda)\, d\lambda],$$

where RF_{SW} is the net incoming shortwave radiation at TOA during the fire period (i.e., radiative forcing), L_{TOA}^{base} and L_{TOA}^{fire} are the observed radiance at the top of atmosphere during base period and fire period, respectively. When integrating with respect to solid angle, we assumed that the ground surface is a Lambert surface (Gristey et al., 2021). As a result, we can see that the radiative forcing over ocean is significantly negative ($-96.7\ \mathrm{Wm^{-2}}$) when the fire is most intense (around 15 September). This might be due to the fact that the ocean has originally lower reflectance in a wide spectrum than that in land, thus, the difference is more pronounced when the fire smoke covers the ocean. Table 2 shows the estimated radiative forcing for Amazon, Angola, Siberia, Australia, and Southeast Asia using the same method as for the California fire. As a result, the radiative forcing is a negative constant at around $-10\ \mathrm{Wm^{-2}}$ over land for every region, which suggest that the instantaneous impact on the radiative forcing might be weak for the burning aerosols over land. However, the smoke spread over the ocean from the fires, resulting in large negative radiative forcing as estimated values of -76.6, $-96.7\ \mathrm{Wm^{-2}}$ for the fires in California and Australia, respectively. Therefore, it is suggested that the main contributor to the difference in radiative forcing might be the difference in the original reflectance of the surface under the fire aerosols.

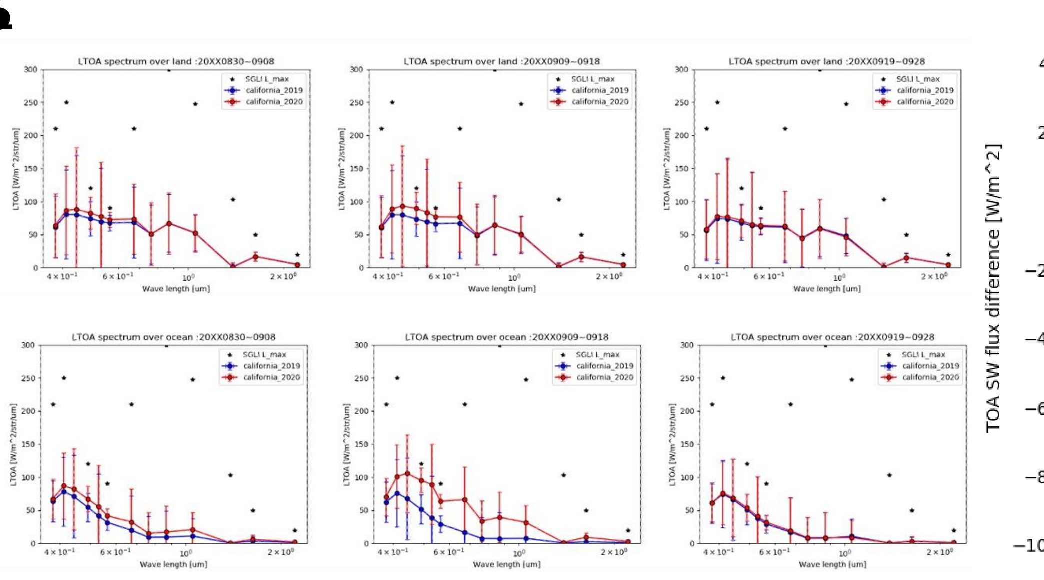

10 days before　　Intense period　　10 days after

Fig. 4 10-days averaged TOA radiance spectra at California (top:land, bottom:ocean)

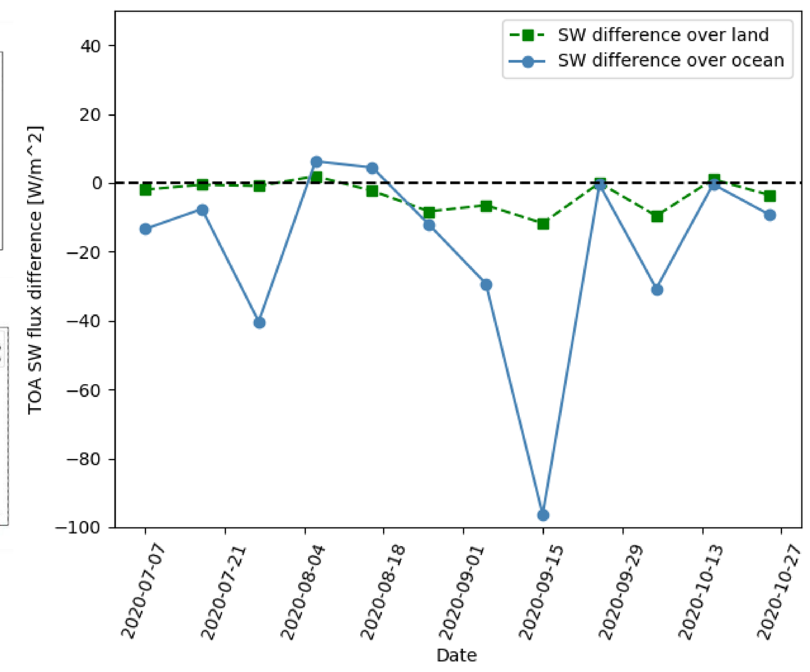

Fig. 5 Variation of the Shortwave RF at California

Table 2 Estimated shortwave RF at each region

Country / State	base period	fire period	RF_{SW} - land $[\mathrm{Wm^{-2}}]$	RF_{SW} - ocean $[\mathrm{Wm^{-2}}]$	RF_{SW} - albedo change $[\mathrm{Wm^{-2}}]$
Amazon	10-19 Sep. 2019	10-19 Sep. 2020	$-12.9(-7.6)$	-	0.04(0.02)
Angola	11-20 Sep. 2020	11-20 Aug. 2020	$-21.1(-12.3)$	-	0.01(0.01)
Australia	31 Dec. 2018 - 9 Jan. 2019	31 Dec. 2019 - 9 Jan. 2020	$-10.9(-6.3)$	$-76.6(-44.1)$	0.19(0.11)
California	9-18 Sep. 2019	9-18 Sep. 2020	$-13.0(-8.0)$	$-96.7(-59.6)$	0.05(0.03)
Siberia	11-20 July 2018	11-20 July 2021	$-7.4(-5.1)$	-	0.18(0.12)
Southeast Asia	11-20 Feb. 2020	11-20 March 2020	$-1.5(-0.9)$	-	0.08(0.05)

Net incoming radiation (RF_{SW} -land and -ocean) is calculated by subtracting shortwave radiation of fire period from that of base (non-fire) period. RF_{SW} -albedo change is the contribution of the land surface albedo changes due to the fire to the net radiative forcing. The values inside the parentheses in the column of RF_{SW} represent the normalized radiation as solar zenith angle of 60°.

In this study, we estimated the regional and instantaneous impacts on the radiative forcing at TOA during fire by aerosol direct effect and surface albedo change, however, it is also needed to be considered aerosol indirect effect on the cloud formation over a longer time span. Besides, regarding the effect of land surface albedo changes, the radiative forcing is positive for a few months after burned, and after that it becomes slightly negative for a few decades as the secondary vegetation with higher reflectance replaces the previous one, according to the global model simulation (Ward et al., 2012). The GCOM-C will continue to observe global climate changes for long term. Thus, when the GCOM-C data is adequately accumulated in the future, we will discuss not only the instantaneous contribution of fires, but also medium and long term influence on the Earth's environment.